ELSEVIER

Chemical Engineering Journal 139 (2008) 408–415

Chemical Engineering Journal

www.elsevier.com/locate/cej

Paper-structured catalyst with porous fiber-network microstructure for autothermal hydrogen production

Hirotaka Koga [a], Shuji Fukahori [a], Takuya Kitaoka [a,*], Mitsuyoshi Nakamura [b], Hiroyuki Wariishi [a]

[a] *Department of Forest and Forest Products Sciences, Graduate School of Bioresource and Bioenvironmental Sciences, Kyushu University, Fukuoka 812-8581, Japan*

[b] *R & D Division, F.C.C. Co. Ltd., Shizuoka 431-1304, Japan*

Received 1 August 2007; received in revised form 22 November 2007; accepted 27 November 2007

Abstract

Copper–zinc oxide catalyst powders were supported on a microstructured matrix composed of ceramic fiber-network by a papermaking technique. As-prepared catalyst materials, called paper-structured catalyst, were applied to the autothermal reforming (ATR) of methanol to produce hydrogen for fuel cell applications. The paper-structured catalyst demonstrated higher methanol conversion and lower undesirable carbon monoxide concentration, as compared with commercial catalysts. Besides, excellent catalyst durability was exhibited by the suppression of Cu sintering during the ATR reaction. The paper-structured catalyst showed remarkable superiority in methanol conversion even in the case of using sintered catalysts. Such features were possibly induced by the unique fiber-network microstructure (average pore size: ca. 20 μm and porosity: ca. 50%) of the paper composites, which may allow the effective transfer of heat and reactants to the catalyst surfaces. The porous paper-structured catalyst is expected as a promising catalytic material for improving the practical performances in the catalytic gas-reforming process.

Keywords: Paper fabrication; Structured catalyst; Porous material; Autothermal reforming; Catalyst durability

1. Introduction

Hydrogen has attracted much attention as an eco-friendly energy source, and the new power generation systems such as polymer electrolyte fuel cells (PEFCs), have promoted effective hydrogen energy usage. Methanol is one of the most promising hydrogen sources since it can be catalytically reformed to hydrogen by using an inexpensive copper–zinc oxide (Cu–ZnO) catalyst at a relatively mild temperature (below 300 °C) [1,2].

Of the various catalytic reforming systems known, the autothermal reforming (ATR) of methanol, which is the combined process of endothermic steam reforming and exothermic partial oxidation, has recently been expected as an efficient energy conversion process as follows [3]:

$$4CH_3OH + 3H_2O + 0.5O_2 \rightarrow 11H_2 + 4CO_2,\ \Delta_r H^{573} \approx 0\ \mathrm{kJ\ mol^{-1}}$$

This reaction is operated autothermally; thus in theory, neither external heating nor cooling is required once the reaction begins.

The catalytic reforming of methanol has mostly been performed over a Cu–ZnO catalyst. Catalysts in powder form are generally inconvenient to handle in practical usage, and are therefore formed into pellets, spheres or rods. However, their catalytic performance is drastically decreased in comparison to that of the original catalyst powder, because the accessibility of gas-phase reactants to the catalytic sites is restricted to the outer surface of the molded solid catalysts [4]. Furthermore, a Cu-based catalyst is easily damaged by heat; catalyst deterioration is a massive drawback, particularly in the ATR process which includes an exothermic reaction [5,6]. Therefore, new types of catalytic materials with high performance are greatly required for effective hydrogen production in the practical reforming process.

The main focus in the development of catalytic materials has been to design the elemental composition and nanometer-scale morphology of the catalyst surface; and thus various catalysts have been upgraded accordingly [7,8]. In particular, extensive

* Corresponding author. Tel.: +81 92 642 2993; fax: +81 92 642 2993.
E-mail address: tkitaoka@agr.kyushu-u.ac.jp (T. Kitaoka).

1385-8947/$ – see front matter © 2007 Elsevier B.V. All rights reserved.
doi:10.1016/j.cej.2007.11.042

effort has been devoted to improve catalyst durability, which is one of the most crucial properties in practical uses [6,9–12]. Patel and Pant [12] reported that the addition of cerium to Cu-based catalysts can improve the catalyst durability by increasing thermal stability via suppression of the nanoscale sintering. However, several significant problems remain in practical cases since the solid catalysts loaded into the reactor frequently cause a high-pressure drop and fluid bypassing, resulting in the remarkable inefficiency of the catalytic reforming process.

In recent years, there has been a major surge of interest in structured catalysts with micrometer-scale pores, which enable the effective diffusion of heat and reactants inside the catalytic material itself during catalytic reactions [13,14]. Several structured catalysts have been developed, e.g. string catalysts, honeycomb catalysts, egg-shell catalysts and metal foam catalysts [3,6,15–18], but further research and developments have been required to put these into practical use.

In our previous reports, Cu–ZnO catalyst powders were successfully formed into paper-like catalyst composites using inorganic fibers as structural components by a papermaking technique [19–21]. As-prepared catalytic materials, called paper-structured catalyst in this study, were easy to fabricate, easy to handle and possessed a porous microstructure derived from the layered fiber-networks. The as-prepared paper-structured catalyst demonstrated efficient hydrogen production: high methanol conversion and low carbon monoxide concentration in comparison to the original Cu–ZnO catalyst powders as well as commercial catalyst pellets. The hydrogen production behavior was also stabilized by using paper-structured catalysts [20]. It was suggested that the unique porous microstructure of the paper composites must play an important role in the ATR performance.

In this study, the catalyst durability of a paper-structured catalyst was compared to that of the original catalyst powder during repeated load testing in the ATR process. X-ray diffractometry (XRD) was conducted to estimate the sintering behavior of the Cu–ZnO catalyst surfaces of the powder-shaped and paper-structured catalysts. The correlation between the ATR performances and Cu crystallite size is discussed in detail.

2. Experimental

2.1. Materials

Commercial Cu–ZnO catalyst pellets (MDC-3; cylindrical shape: 3 mm in diameter and 3 mm in height; SÜD-CHEMIE, Ltd.) were used, and some were pulverized into powders with 100 mesh-pass size. Pulp fibers as a tentative supporting matrix in the paper fabrication process were obtained by refining commercial bleached hardwood kraft pulp to 300 ml of Canadian Standard Freeness [22] with a Technical Association of the Pulp and Paper Industry (TAPPI) standard beater [23]. Ceramic fibers (IBIWOOL, IBIDEN, Ltd.) were cut into an average length of ca. 0.5 mm using a four-flute end mill. Two types of flocculants were used as retention aids: cationic polydiallyldimethylammonium chloride (PDADMAC; molecular weight: ca. 3×10^5; charge density: 5.5 meq g^{-1}; Aldrich, Ltd.) and anionic polyacrylamide (A-PAM, HH-351; molecular weight: ca. 4×10^6; charge density: 0.64 meq g^{-1}; Kurita, Ltd.). An alumina sol (Snowtex 520, Nissan Chemicals, Ltd.) was used as a binder to improve the physical strength of the catalyst paper after calcination.

2.2. Preparation of paper-structured catalyst

A paper-structured catalyst was prepared according to our previous reports [19–21]. The outline of a papermaking procedure is summarized as follows. A ceramic fiber/water suspension (1.0%, w/v) containing Cu–ZnO catalyst powder was mixed with PDADMAC (0.5 wt% per solids), alumina sol and A-PAM (0.5 wt% per total solids) in that order, with each step being carried out at an interval of 3 min. The mixture was added to a pulp fiber suspension (0.125%, w/v), and solidified by dewatering using a 200-mesh wire according to the TAPPI Test Methods T205 [24]. The handsheets were dried in an oven at 105 °C for 1 h, following pressing at 350 kPa for 3 min. The resulting paper-structured catalyst consisted of Cu–ZnO catalyst powders (1.5 g), ceramic fibers (5.0 g), alumina sol (0.50 g) and pulp fibers (0.00 or 0.25 g). The paper-structured catalyst obtained was thermally treated at 350 °C for 12 h to remove pulp fibers and to improve the physical strength by binder sintering.

2.3. ATR performance test

The schematic diagram of the ATR reactor used in this study is illustrated in Fig. 1. Ten disc-shaped paper-structured catalysts with a thickness of 1 mm were stacked one on top of each other (8×10^3 mm^3) and placed on a perforated support plate inside a stainless steel cylindrical reactor. The catalyst discs were packed against the inner wall of the reactor, in order to make good contact with the inner surface of the reactor. Catalyst powders or pellets were mixed with 100-mesh pass ceramic powders to adjust the occupied volume to 8×10^3 mm^3 and packed in the cylinder in which a glass fiber filter (GA-55, ADVANTEC, Ltd.)

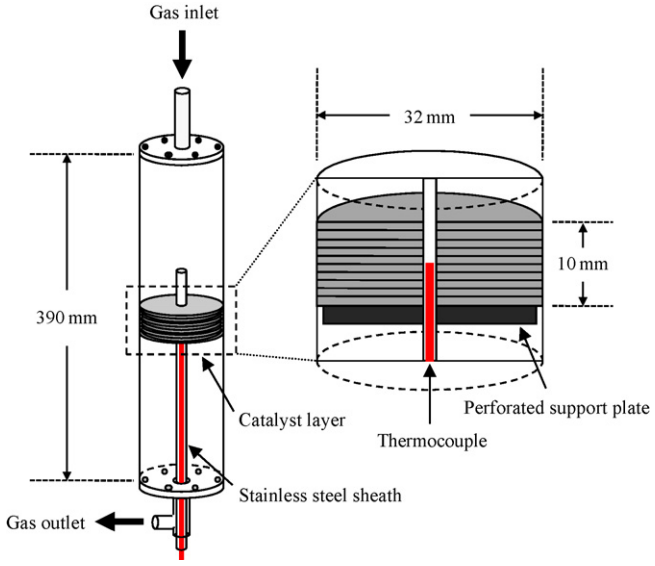

Fig. 1. Schematic diagram of the ATR reactor.

was set on the perforated support plate. The amount of Cu–ZnO catalyst was set at 0.6 g in each case, regardless of the catalyst shape. The outline of the gas flow system whose all connections are completely sealed with copper O-rings is given in our previous report [19]. Prior to the ATR process, the reduction of the Cu–ZnO catalyst was carried out in the reactor with flowing hydrogen at 250 °C for 1.5 h followed by a complete purge of all the flow lines with nitrogen for 30 min. Subsequently, a mixed gas with methanol/water/oxygen (molar ratio: 1.00/1.50/0.125) was fed into the reactor at a constant space velocity of 1130 h^{-1} (150 ml/min). Methanol and water were supplied to a mixing box by two plunger pumps (LP-6300, Lab-Quatec, Ltd.) and the mixture was vaporized at 200 °C. Oxygen flow was adjusted by a mass flow controller (HM1141A, HEMMI Slide Rule, Ltd.). The temperature of inlet gas was kept at 200 °C with a flexible ribbon heater. Exhaust back pressure of the gas flow line was monitored online by a pressure sensor mounted at the top of the reactor. The ATR process was conducted at a reaction temperature of 250 °C in the continuous heat supply system equipped with a mantle heater. The gas generated in the ATR reaction was passed through a cold trap in an ice bath; then the unreacted methanol and water residues were separated from the gaseous components. After 2 h of the ATR operation, the flow rate of the generated gas and the internal temperature of the reactor were simultaneously monitored every second for 3 h using a mass flow meter (3810S, KOFLOC, Ltd.) and a thermocouple inserted in the middle layer of the catalyst samples, respectively. The methanol conversion was calculated by averaging the gas flow rate as compared to the theoretical flow rate at maximum (126 standard cubic centimeters per minute; SCCM), by taking the unreacted methanol and water in the cold trap into consideration. The major gaseous products, hydrogen (ca. 73%) and carbon dioxide (ca. 27%), were analyzed online using a gas chromatograph (GC)-thermoconductivity detector with a Porapak-Q column (3 mm × 2 m, Shinwa Chemical Industries, Ltd.). Carbon monoxide as a minor by-product (less than 1%) was measured by a GC-flame ionization detector with a Porapak-Q column after the complete conversion of carbon monoxide to methane by an online methanizer (MTN-1, Shimadzu, Ltd.). The catalyst durability was evaluated by the variations in the methanol conversion during the five-cycles ATR test: the sequential procedure of catalyst reduction (1.5 h), line purging (30 min) and ATR reaction (5.0 h) as a one-cycle test. All measurements were performed at least three times and standard deviations were obtained.

2.4. Other analyses

The catalyst content of the paper composites was determined by atomic absorption analysis using a Shimadzu AA-6600F apparatus. The concentration of Cu^{2+} eluted from the Cu–ZnO catalyst with 35% nitric acid was quantified through flame atomic absorbance. Other inorganic materials were measured gravimetrically after calcination at 700 °C for 20 min, by taking weight loss into consideration. Surface observation of the paper-structured catalyst was performed by scanning electron microscopy (SEM, JSM-5600, JEOL, Ltd.). The electron accelerating voltage was set at 10 kV. Mercury intrusion analysis was carried out using a Poremaster 33P (YUASA IONICS, Ltd.) to evaluate the pore diameter and porosity of the catalyst samples. The pore size distribution was obtained from the pressure-cumulative mercury intrusion volume curve normalized by the catalyst weight. The XRD of the samples was conducted using an XD-D1 X-ray diffractometer (Shimadzu, Ltd.) with Ni-filtered Cu Kα radiation (λ = 1.5418 Å) with a scanning angle (2θ) of 30–60° at a voltage of 30 kV and a current of 40 mA. The diffraction pattern was identified from the results of the previous reports [25–27]. The Scherrer formula was used to estimate the Cu crystallite size on the basis of the full width at half maximum of Cu(1 1 1) reflection (2θ = 43°) [27], by using an XRD-6100/7000 v5.21 software (Shimadzu, Ltd.).

3. Results and discussion

3.1. Paper-structured catalyst prepared by a papermaking technique

Fig. 2 shows optical images of 100-mesh pass Cu–ZnO catalyst powders, commercial catalyst pellets and two pieces of paper-structured catalyst for ATR performance testing. The paper-structured catalyst was strengthened by sintering with an alumina sol binder and the resulting paper having the appearance of flexible cardboard, was found to be notably easier to handle. As we previously reported, the retention of inorganic materials including catalyst powders reached more than 90% in the dual polymer retention system [19–21,28–32]. Fig. 3 shows the SEM images of the surfaces of paper-structured catalysts. Before calcination, the dense fiber-mix material composed of pulp and ceramic fibers was observed as shown in Fig. 3a. Pulp fibers, which are a tentative matrix of the wet-state paper web, play an essential role in providing the physical strength of paper composites before binder sintering. After calcination, the organic pulp fibers were completely removed, leaving small catalyst powders on the ceramic fiber-networks (Fig. 3b). Fig. 4 profiles the pore size distribution of the catalyst powder and paper-structured catalyst, as determined by the mercury intrusion method. A clear peak around 20 μm was observed only for the paper-structured catalyst, and not for the catalyst powder. The porosity of the paper-structured catalyst reached up to ca. 50%. It was estimated from the SEM image (Fig. 3b) that the micrometer-scale pores inside the paper-structured catalyst were derived from the layered ceramic fiber-networks.

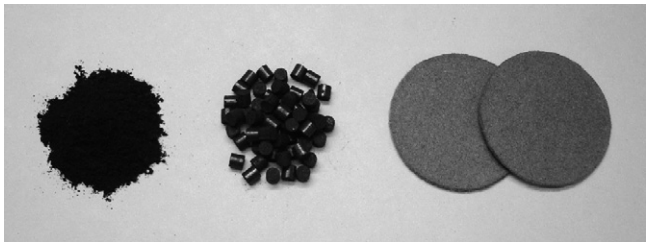

Fig. 2. Optical images of Cu–ZnO catalyst powder (left), commercial pellet-type catalyst (middle) and paper-structured catalyst (right).

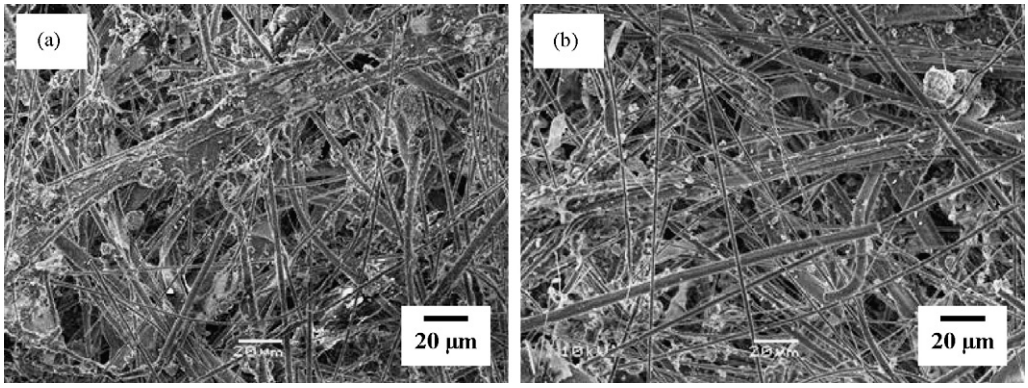

Fig. 3. SEM images of the surfaces of a paper-structured catalyst; before (a) and after (b) calcination.

3.2. ATR Performance of paper-structured catalyst

Table 1 compares the ATR performance of the catalyst powder, pellet-type catalyst and paper-structured catalyst at a gas space velocity of 1130 h^{-1}. The methanol conversion performed with the paper-structured catalyst was comparable with that of the original catalyst powder, surpassing by far that of the commercial pellet-type catalyst. In general, the carbon monoxide by-product acts as a catalytic poison for the Pt anode electrocatalyst of PEFCs [33]; however in the methanol reforming process, carbon monoxide is inevitably produced by the reverse water–gas shift reaction in which the reformed gas components, hydrogen and carbon dioxide, are converted endothermically to water and carbon monoxide ($H_2 + CO_2 \rightarrow H_2O + CO$, $\Delta_r H^{298} = +41\ kJ\ mol^{-1}$) [2,4,34]. Hence, the concentration of carbon monoxide in the reformed gas often tends to increase with an increase in the methanol conversion. In the case of the paper-structured catalyst, however, the carbon monoxide concentration was drastically reduced to around 3000 ppm, which was two-thirds that generated using catalyst pellets and less than half that produced with catalyst powder. In all of the ATR performance tests, both the actual amount of Cu–ZnO catalyst and the occupied volume in the reactor were adjusted to be identical. Besides, the simple mixing of alumina sol binder with catalyst powder or pellet led to an obvious reduction in methanol conversion, indicating that the alumina components, which were added to enhance the physical strength of paper composites, must be a negative factor for the ATR efficiency due to the partial coverage of the catalyst surface. Therefore, such results strongly suggested that the unique microstructure, i.e. fiber-network pores, made a great contribution to improve the catalytic ATR performance.

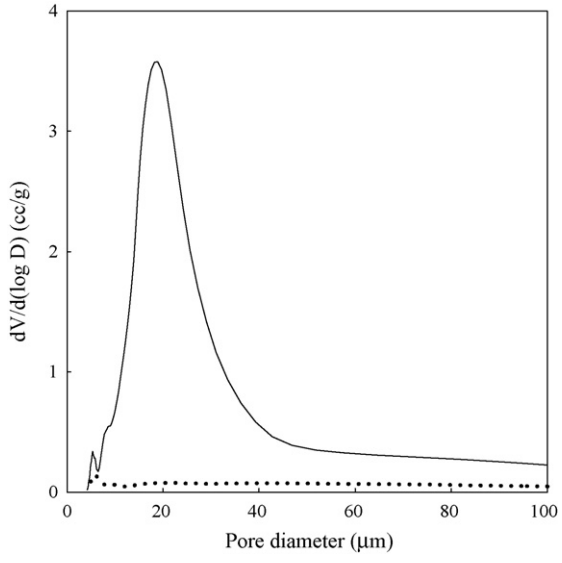

Fig. 4. Pore size distribution of catalyst samples; catalyst powder (dotted line) and paper-structured catalyst (solid line).

3.3. Monitoring of ATR reaction behavior

Fig. 5 profiles the flow rate of the reformed gas and the internal temperature of the reactor over time for the catalyst powder, pellets and paper at a gas space velocity of 1130 h^{-1}. The gas flow rate is presented in the standard cubic centimeters per minute parameter. In the case of the catalyst powder and pellets, some large oscillations in the gas flow were observed with large variations in the internal temperature. These results indicated that the solid catalyst loading presumably caused the localized flow, and also the heat variations in the cylindrical reactor due to the heterogeneous sample packing: a drastic drop in the reaction temperature directly induced a remarkable reduction in the methanol conversion. Furthermore, such a channeling phenomenon is expected to have some impact on the carbon monoxide formation by the endothermic reverse water–gas shift reaction: the localization of heat and the reformed gas components, hydrogen and carbon dioxide, around the Cu–ZnO catalysts may promote the formation of carbon monoxide in the local equilibrium states. On the other hand, the paper-structured catalyst demonstrated a relatively stable ATR behavior, and

Table 1
ATR performances; reaction temperature: 250 °C, gas space velocity: 1130 h^{-1}

Catalyst shape	Methanol conversion (%)	CO concentration (ppm)
Catalyst powder	88.7 ± 4.8	6700 ± 800
Pellet-type catalyst	46.3 ± 2.0	4500 ± 200
Paper-structured catalyst	88.9 ± 0.8	3100 ± 300

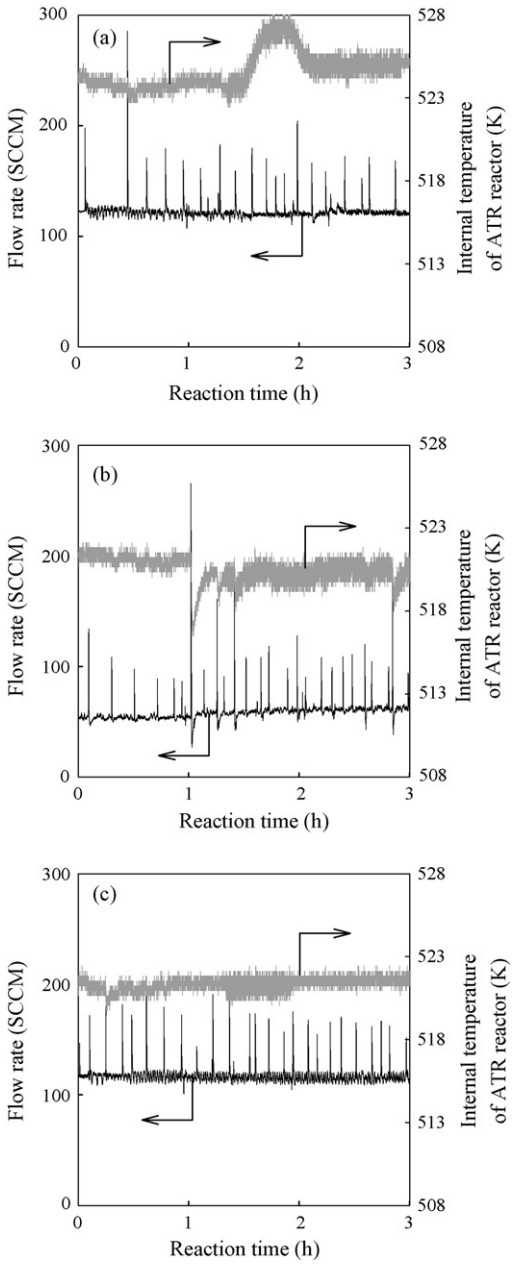

Fig. 5. Hydrogen production behavior; catalyst powder (a), pellet (b), paper-structured catalyst (c); flow rate (black lines) and internal temperature (gray lines).

in particular the internal temperature of the reactor remained almost stable during 3 h of the ATR reaction. The paper-structured catalyst had a porous fiber-network on which the catalyst particles are well scattered as shown in Fig. 3b. For the nanometer-sized pores, there was no distinct difference among the catalyst powder, pellets and paper [19]. Therefore, the unique porous microstructure of the paper composites must make for the uniform gas flow, resulting in the uniform ATR reaction.

We have previously reported the ATR performances of these catalyst samples at a gas space velocity of 2260 h^{-1} [20]. With respect to the hydrogen production behavior, there was not much difference between 1130 h^{-1} and 2260 h^{-1}. On the other hand, the carbon monoxide concentration of the catalyst powder increased from ca. 5000 ppm to ca. 7000 ppm when a gas space velocity decreased by half from 2260 h^{-1} to 1130 h^{-1}, since it is well known that the formation of the carbon monoxide by-product tends to increase with decreasing gas space velocity, owing to the longer residence time around the catalyst surfaces [6]. However, the carbon monoxide concentration of the paper-structured catalysts made a little difference in both 1130 h^{-1} and 2260 h^{-1}. Continuous back pressure was not significantly detected in all test cases, and thus the gas back pressure was low as to be neglected within the measurable limit (10 kPa). Therefore, there may be nearly no difference in the gas resistance among catalyst powder, pellet and paper-structured catalyst. However, the solid catalyst loading presumably causes the localized flow in the catalyst layer (Fig. 5). On the other hand, the paper-structured catalyst may provide a uniform flow into the porous catalyst layer, leading to the stable and high methanol conversion in the fiber-network microstructure. Many researchers have pointed out that the favorable and uniform accessibility of the reactants to catalytic sites is of great importance to achieve both a high catalytic efficiency and selectivity in various catalytic processes [16,35]. Thus, such interesting phenomena for paper-structured catalysts would imply that they provide a degree of desirable gas accessibility to the catalyst surfaces by improving the flow of reactants and reformed gas inside the fiber-network microstructure, resulting in a higher methanol conversion, more efficient hydrogen production and a remarkable suppression of carbon monoxide by-production.

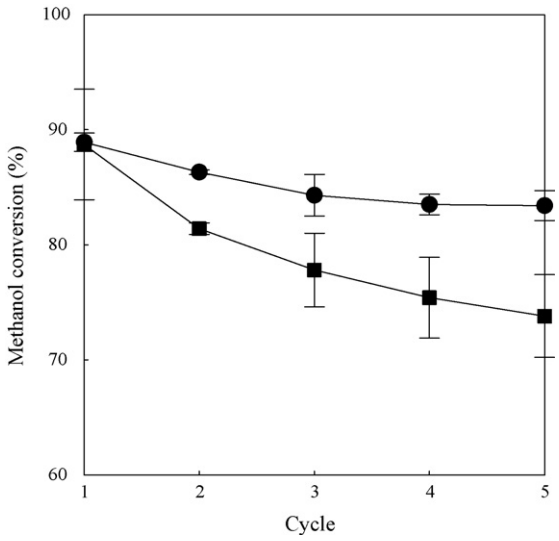

Fig. 6. Catalyst durability for methanol conversion; catalyst powder (closed squares) and paper-structured catalyst (closed circles).

3.4. Catalyst durability performance

Catalyst durability is one of the requisite properties for practical catalyst applications to ensure their repeated use; and thus a number of repeated load tests were reported [36,37]. Fig. 6 compares the durability performance between a catalyst powder and paper-structured catalyst with respect to the variations in the methanol conversion during the five-cycles ATR test. Dur-

ing the first cycle, both catalysts demonstrated a high methanol conversion around 90% (also see Table 1). In the case of the catalyst powder, however, the methanol conversion was drastically decreased as the test cycle progressed: the decrease in the methanol conversion was ca. 17% after the five-cycles ATR test. It is well known that Cu-based catalysts are highly sensitive to thermal sintering [5]. Lattner and Harold [38] proposed that critical to the catalyst durability is the balancing of the endothermic reforming and exothermic oxidation reactions in the ATR process to avoid excessive temperature. In the conventional reactors with randomly packed catalytic beds, however, channeling effects which give the eccentric flow of heat and reactants frequently must lead to the heterogeneous thermal environment inside the catalyst layers, as shown in Fig. 5a and b. Thus, it was assumed that the catalyst powder packed into the reactor induced a hot spot formation, resulting in deactivation of the catalyst because of critical Cu sintering. On the other hand, the paper-structured catalyst showed a high durability performance: the decrease in the methanol conversion was only ca. 6% after the five-cycles reforming test. As shown in Fig. 5c, the thermal environment inside the paper-structured catalyst was obviously stable; thus it was suggested that an undesirable hot spot formation was mitigated to some extent by the aforementioned paper-specific structural effect.

In the conventional ATR process, most of the reaction heat is generated at the reactor entrance (the top-layer catalysts) due to the fast exothermic methanol oxidation reaction, resulting in the hot spot formation at the front part of the catalyst layer [6,38]. In this study, the reaction temperatures were roughly measured at three vertical positions, i.e. top, middle and bottom of the catalyst layers mounted in the ATR reactor (Fig. 1). The averaged temperature distribution of paper-structured catalyst was relatively uniform as compared with that of catalyst powders: the temperature gradients were 4 K (from 251 °C to 247 °C) for paper-structured catalyst and 6 K (from 252 °C to 246 °C) for catalyst powders. Patcas et al. [39] suggested that the foam structure, which consists of a network of interconnected solid struts building cavities that communicate through windows, allowed the effective heat transport by convection and radiation. It was presumed that the unique fiber-network microstructure of the paper-structured catalyst led to the similar heat transfer phenomenon.

XRD analysis was conducted to elucidate the changes in the crystalline structures of the Cu–ZnO catalyst both before and after the five-cycles ATR test. Representative XRD profiles of the catalyst powder and paper-structured catalyst are given in Fig. 7. Of various specific reflections, the main peak of Cu at 43°, which is ascribed to Cu(1 1 1) was applied to the crystallite size calculated by the Scherrer formula [27]. Table 2 summarizes the Cu crystallite sizes of the catalyst powder and paper-structured catalyst before and after the five-cycles ATR test. In the case of the catalyst powder, the Cu crystallite size increased by 3.1 nm (from 9.6 nm to 12.7 nm) after the five-cycles test, indicating the obvious Cu sintering [9,25,27]. On the contrary, the Cu crystallite size of the paper-structured catalyst remained almost unchanged, albeit slightly increased by 0.3 nm (from 13.6 nm to 13.9 nm). However, it

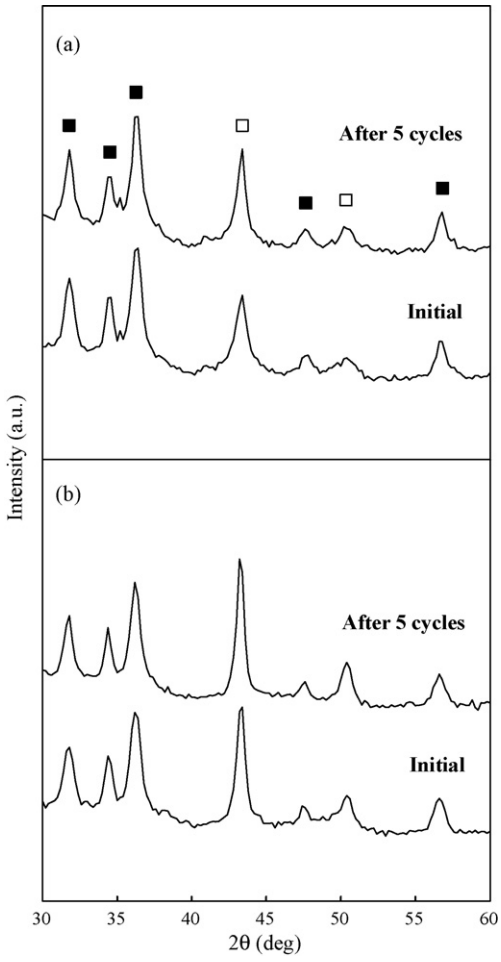

Fig. 7. XRD profiles of Cu–ZnO catalyst powder (a) and paper-structured catalyst (b); (□) Cu and (■) ZnO.

should be noted that the Cu crystallite size of the paper-structured catalyst was evidently larger at the initial state than that of the catalyst powder. This result suggested that the paper calcination led to Cu sintering, probably owing to the combustion heat of organic pulp fibers; thus it must be considered that the Cu–ZnO catalyst in the paper-structured catalyst was somewhat limited to further sintering in the ATR reaction.

Indeed, pulp fibers play a key role in the fabrication of paper-structured catalysts, and thus it is very difficult to make them without pulp fibers in practical situations. However, in this study,

Table 2
Cu crystallite size before and after five-cycles ATR test

Catalyst shape	Pulp[a]	Cu crystallite size (nm)	
		Initial	After five cycles
Catalyst powder	+	13.2 ± 0.4	14.7 ± 0.1
	−	9.6 ± 0.4	12.7 ± 0.6
Paper-structured catalyst	+	13.6 ± 0.8	13.9 ± 0.4
	−	9.4 ± 0.7	10.4 ± 0.6

[a](+): Each sample was beforehand calcined at 350 °C for 12 h in the presence of pulp fibers. (−): Catalyst powder was used in its original state, and paper-structured catalyst prepared without pulp fibers was calcined at 350 °C for 12 h.

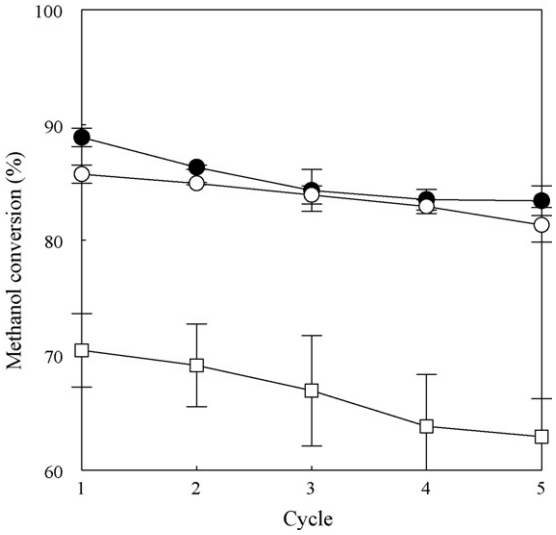

Fig. 8. Catalyst durability for methanol conversion; catalyst powder (open squares) and paper-structured catalyst: pulp addition (closed circles) and pulp-free (open circles). Catalyst powder was beforehand mixed with pulp, and calcined at 350 °C for 12 h in a similar manner to that for preparing the paper-structured catalyst. Closed circles are identical with those in Fig. 6.

a pulp-free paper-structured catalyst was experimentally prepared without adding any pulp fibers in order to eliminate the predicted negative effect on the Cu–ZnO catalyst. As-prepared pulp-free catalyst paper was calcined at 350 °C for 12 h and subjected to XRD analysis. As shown in Table 2, the Cu crystallite size of the pulp-free catalyst paper was ca. 9.4 nm at the initial state, being almost the same as that of the original powder (9.6 nm); and thus it was suggested that the calcination in the absence of pulp fibers had little or no influence on the Cu sintering. In contrast, catalyst powder mixed with pulp fibers, followed by calcination in a similar way, showed obvious Cu sintering, since the Cu crystallite size increased by 3.6 nm from 9.6 nm to 13.2 nm (see Table 2). These results rationalized that the combustion heat of pulp fibers must cause undesirable Cu sintering. Subsequently, pulp-free catalyst paper and catalyst powder calcined in the presence of pulp fibers were applied to the five-cycles ATR test, followed by XRD analysis. In Fig. 8 and Table 2, the pulp-free catalyst paper demonstrated a high durability performance, in accordance with that observed for the paper-structured catalyst prepared using pulp fibers: the decrease in the methanol conversion was within ca. 5% during the five-cycles test, and then the increase in Cu crystallite size was ca. 1.0 nm. On the other hand, catalyst powder calcined in the presence of pulp fibers showed poor methanol conversion (ca. 70%) and durability: the decrease in the methanol conversion was ca. 11%, and the increase in Cu crystallite size was ca. 1.5 nm. In the same case, the paper-structured catalyst with added pulp was ca. 6% and 0.3 nm, respectively, displaying a high methanol conversion (ca. 90%), although the Cu crystallite size at the initial state was almost the same in both cases: paper-structured catalyst and catalyst powder calcined with pulp fibers.

The paper-structured catalyst possessed excellent durability, as well as catalytic efficiency and selectivity, properties which were caused neither by the element composition nor

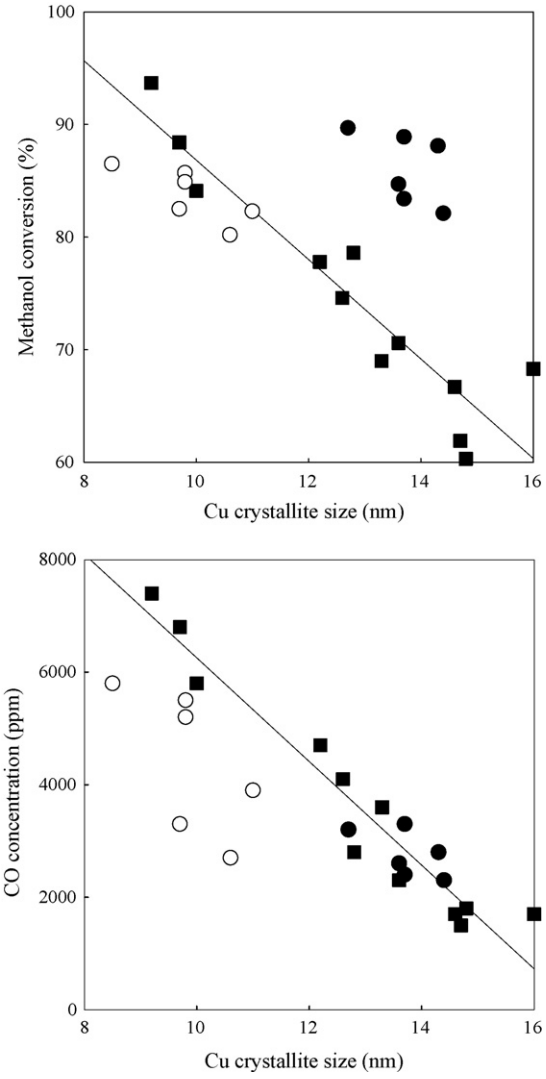

Fig. 9. Correlation between ATR performances and Cu crystallite size; catalyst powder (closed squares) and paper-structured catalyst: pulp addition (closed circles) and pulp-free (open circles).

by the nanometer-scale morphology of the catalyst surface, but by the fiber-network matrix microstructure. Such features were possibly involved in the paper-specific effect; namely, the unique fiber-network microstructure provides an effective catalytic environment inside the catalyst layer, resulting in the suppression of hot spot formation (see Fig. 5c), as well as the formation of the carbon monoxide by-product (see Table 1).

3.5. Effect of paper structure on catalytic efficiency

Paper-structured catalysts prepared using pulp fibers demonstrated a high methanol conversion of ca. 90% at the first cycle, although the Cu–ZnO catalyst was greatly deteriorated due to the combustion heat of the pulp fibers, as shown in Tables 1 and 2. Fig. 9 summarizes the correlation between the ATR performance and Cu crystallite size with regard to the catalyst powder and paper-structured catalysts. In the case of the catalyst powder, the Cu crystallite size varied with calcination of the pulp fibers present. The methanol conversion capability of the catalyst pow-

der was markedly decreased as the Cu crystallite size increased. It has been reported that an increase in Cu crystallite size, i.e. Cu sintering, is closely related to a decrease in the catalytic reactivity [9,25]. Methanol conversion by using a catalyst powder was only ca. 70% at the Cu crystallite size of ca. 14 nm, compared to ca. 90% at ca. 10 nm in the initial state. Of special note: the methanol conversion achieved using paper-structured catalysts was obviously high in comparison to that with catalyst powder at the same catalyst state, while the concentration of carbon monoxide produced was almost the same in both cases. These results indicate that the porous paper structure dramatically improved the practical performance of the Cu–ZnO catalyst. Furthermore, the paper-structured catalyst prepared using pulp fibers demonstrated an equal or slightly higher methanol conversion capability than the pulp-free catalyst paper, although the catalyst itself deteriorated in the pulp-added catalyst paper. Thus, it was also suggested that the ceramic fiber-network microstructure formed by the removal of the pulp fiber template from the paper composites may contribute to the certain enhancement of apparent catalytic efficiency. There would be much interest in further research and development for the catalytic performance of paper-structured catalysts by controlling the porous fiber-network structure.

4. Conclusions

A paper-structured catalyst with porous fiber-network microstructure was successfully prepared using a papermaking technique. In the ATR process, the paper-structured catalyst demonstrated high methanol conversion and low carbon monoxide concentration in comparison to not only the commercial catalyst pellets but also to the original catalyst powder. Besides, the durability of the Cu–ZnO catalyst was remarkably improved, and a high methanol conversion remained almost unchanged during the repeated ATR test. Such features were possibly attributed to the structural effect of the paper-specific pores providing a uniform flow of reactants and a homogeneous heat environment inside the catalyst layer, contributing to some improvement for the catalyst durability as well as catalytic efficiency and selectivity. Thus, the paper-structured catalyst easy to fabricate by an established high-speed and low-cost papermaking technique is expected to provide both practical utility and high efficiency in the catalytic gas-reforming process.

Acknowledgements

This research was supported by Research Fellowships of the Japan Society for the Promotion of Science for Young Scientists (H.K. and S.F.) and by an Industrial Technology Research Grant Program in 2003 from the New Energy and Industrial Technology Development Organization (NEDO) of Japan (T.K.).

References

[1] S. Nagano, H. Miyagawa, O. Azegami, K. Ohsawa, Energy Conv. Manag. 42 (2001) 1817–1829.
[2] J. Agrell, H. Birgersson, M. Boutonnet, J. Power Sources 106 (2002) 249–257.
[3] C. Horny, L. Kiwi-Minsker, A. Renken, Chem. Eng. J. 101 (2004) 3–9.
[4] H. Purnama, T. Ressler, R.E. Jentoft, H. Soerijanto, R. Schlögl, R. Schomäcker, Appl. Catal. A: Gen. 259 (2004) 83–94.
[5] M.V. Twigg, M.S. Spencer, Appl. Catal. A: Gen. 212 (2001) 161–174.
[6] C. Horny, L. Kiwi-Minsker, A. Renken, Catal. Today 120 (2007) 45–53.
[7] B. Lindström, L.J. Pettersson, P.G. Menon, Appl. Catal. A: Gen. 234 (2002) 111–125.
[8] Y. Zhang, M. Koike, R. Yang, S. Hinchiranan, T. Vitidsant, N. Tsubaki, Appl. Catal. A: Gen. 292 (2005) 252–258.
[9] T. Shishido, M. Yamamoto, I. Atake, D. Li, Y. Tian, H. Morioka, M. Honda, T. Sano, K. Takehira, J. Mol. Catal. A 253 (2006) 270–278.
[10] T. Kanazawa, Appl. Catal. B: Environ. 65 (2006) 185–190.
[11] S. Kameoka, T. Tanabe, A.P. Tsai, Catal. Lett. 100 (2005) 89–93.
[12] S. Patel, K.K. Pant, J. Power Sources 159 (2006) 139–143.
[13] N. Dupont, G. Germani, A.C. van Veen, Y. Schuurman, G. Schäfer, C. Mirodatos, Int. J. Hydrogen Energy 32 (2007) 1443–1449.
[14] L.L. Makarshin, V.N. Parmon, Russ. J. Gen. Chem. 77 (2007) 676–684.
[15] V. Tomašić, F. Jović, Appl. Catal. A: Gen. 311 (2006) 112–121.
[16] F. Patcas, W. Krysmann, Appl. Catal. A: Gen. 316 (2007) 240–249.
[17] H. Yu, H. Chen, M. Pan, Y. Tang, K. Zeng, F. Peng, H. Wang, Appl. Catal. A: Gen. 327 (2007) 106–113.
[18] B. Lindström, J. Agrell, L.J. Pettersson, Chem. Eng. J. 93 (2003) 91–101.
[19] S. Fukahori, T. Kitaoka, A. Tomoda, R. Suzuki, H. Wariishi, Appl. Catal. A: Gen. 300 (2006) 155–161.
[20] H. Koga, S. Fukahori, T. Kitaoka, A. Tomoda, R. Suzuki, H. Wariishi, Appl. Catal. A: Gen. 309 (2006) 263–269.
[21] S. Fukahori, H. Koga, T. Kitaoka, A. Tomoda, R. Suzuki, H. Wariishi, Appl. Catal. A: Gen. 310 (2006) 138–144.
[22] Tech. Assoc. Pulp Pap. Ind. Test Methods, 1997, T227.
[23] Tech. Assoc. Pulp Pap. Ind. Test Methods, 1997, T200.
[24] Tech. Assoc. Pulp Pap. Ind. Test Methods, 1997, T205.
[25] T. Shishido, M. Yamamoto, D. Li, Y. Tian, H. Morioka, M. Honda, T. Sano, K. Takehira, Appl. Catal. A: Gen. 303 (2006) 62–71.
[26] J.-D. Grunwaldt, A.M. Molenbroek, N.-Y. Topsøe, H. Topsøe, B.S. Clausen, J. Catal. 194 (2000) 452–460.
[27] M.M. Günter, T. Ressler, R.E. Jentoft, B. Bems, J. Catal. 203 (2001) 133–149.
[28] H. Ichiura, T. Kitaoka, H. Tanaka, Chemosphere 50 (2003) 79–83.
[29] H. Ichiura, T. Kitaoka, H. Tanaka, Chemosphere 51 (2003) 855–860.
[30] H. Ichiura, T. Kitaoka, H. Tanaka, J. Mater. Sci. 38 (2003) 1611–1615.
[31] S. Fukahori, H. Ichiura, T. Kitaoka, H. Tanaka, Environ. Sci. Technol. 37 (2003) 1048–1051.
[32] S. Fukahori, H. Ichiura, T. Kitaoka, H. Tanaka, Appl. Catal. B: Environ. 46 (2003) 453–462.
[33] T. Utaka, K. Sekizawa, K. Eguchi, Appl. Catal. A: Gen. 194–195 (2000) 21–26.
[34] T. Gu, W.-K. Lee, J.W. Van Zee, Appl. Catal. B: Environ. 56 (2005) 43–49.
[35] I.Z. Ismagilov, R.P. Ekatpure, L.T. Tsykoza, E.V. Matus, E.V. Rebrov, M.H.J.M. de Croon, M.A. Kerzhentsev, J.C. Schouten, Catal. Today 105 (2005) 516–528.
[36] N.S. Chaubai, M.R. Sawant, Catal. Commun. 7 (2006) 443–449.
[37] T. Osawa, M. Maegawa, M. Yoshihisa, M. Kobayashi, T. Harada, O. Takayasu, Catal. Lett. 107 (2006) 83–88.
[38] J.R. Lattner, M.P. Harold, Catal. Today 120 (2007) 78–89.
[39] F.C. Patcas, G.I. Garrido, B. Kraushaar-Czarnetzki, Chem. Eng. Sci. 62 (2007) 3984–3990.